

1135

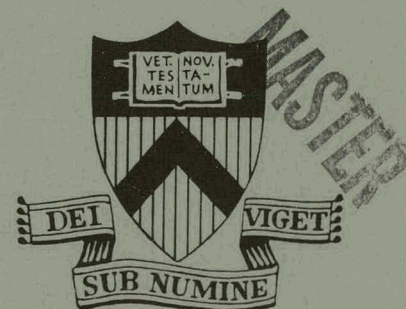
JULY 1975

MATT-1135

A CHRONICLE OF ION-CURRENT  
INSTABILITIES  
- OLD AND NEW

R. W. LANDAU

PLASMA PHYSICS  
LABORATORY



PRINCETON UNIVERSITY  
PRINCETON, NEW JERSEY

This work was supported by U. S. Atomic Energy Commission Contract AT(11-1)-3073. Reproduction, translation, publication, use, and disposal, in whole or in part, by or for the United States Government is permitted.

DISTRIBUTION OF THIS DOCUMENT UNLIMITED

## **DISCLAIMER**

**This report was prepared as an account of work sponsored by an agency of the United States Government. Neither the United States Government nor any agency Thereof, nor any of their employees, makes any warranty, express or implied, or assumes any legal liability or responsibility for the accuracy, completeness, or usefulness of any information, apparatus, product, or process disclosed, or represents that its use would not infringe privately owned rights. Reference herein to any specific commercial product, process, or service by trade name, trademark, manufacturer, or otherwise does not necessarily constitute or imply its endorsement, recommendation, or favoring by the United States Government or any agency thereof. The views and opinions of authors expressed herein do not necessarily state or reflect those of the United States Government or any agency thereof.**

## **DISCLAIMER**

**Portions of this document may be illegible in electronic image products. Images are produced from the best available original document.**

A CHRONICLE OF ION-CURRENT INSTABILITIES - OLD AND NEW

Ronald W. Landau  
Plasma Physics Laboratory, Princeton University  
Princeton, New Jersey 08540

and

Queens College of the City University of New York  
Flushing, New York 11367

ABSTRACT

For counter-streaming ion currents along a uniform magnetic field, a purely growing instability exists with a growth rate as high as 16 times the ion gyrofrequency. When the streaming ions are only 1% of the stationary ions, the growth rate is still 4 times the gyrofrequency, but the real part is near the lower hybrid frequency. These instabilities are in addition to the Drummond-Rosenbluth ion mode. Finite  $\beta$  effects increase the growth rate and can be important for  $\beta > 10^{-4}$ . In all this,  $T_{\parallel,+} = T_{\parallel,-}$  and  $T_{\perp} = 0$ .

NOTICE

This report was prepared as an account of work sponsored by the United States Government. Neither the United States nor the United States Energy Research and Development Administration, nor any of their employees, nor any of their contractors, subcontractors, or their employees, makes any warranty, express or implied, or assumes any legal liability or responsibility for the accuracy, completeness or usefulness of any information, apparatus, product or process disclosed, or represents that its use would not infringe privately owned rights.

DISTRIBUTION OF THIS DOCUMENT UNLIMITED

There is considerable interest in using neutral beams to heat plasmas in a new generation of Tokamaks<sup>1,2</sup> to achieve marginal power production. The neutral beams themselves are very monoenergetic<sup>3</sup> and when converted to ions produce beams that are also probably rather monoenergetic<sup>4</sup>. The proposals<sup>1,2</sup> envisage injection of counter-streaming ions tangent to the magnetic field. The earlier proposals<sup>1</sup> envisage a beam of density much less than the warm plasma, but more recent suggestions<sup>2</sup> have pointed out that less energetic beams are required if one preferentially removes low energy ions, so that the "plasma" consists of two counterstreaming ion beams. Due to the importance of the above ideas it seems appropriate to examine carefully the instabilities of ion beams flowing along the magnetic field.

### 1.1 ZERO PERPENDICULAR TEMPERATURE ( $T_{\perp} = 0$ )

To this end we have extended our previous equations<sup>5,6</sup> giving the dispersion relations for a  $T_{\perp} = 0$  plasma to include streaming along the uniform magnetic field  $\vec{B}_0$ , which lies in the  $z$  direction. The temperature is Maxwellian along the field. These equations have also been given by Stix<sup>7</sup> although we have preferred to work with our notation<sup>8</sup>.

We assume  $\vec{k} = k_{\perp} \hat{i} + k_{\parallel} \hat{k}$  is the wave vector and consider two ion beams of density  $\epsilon n$  each, with equal and opposite velocities  $V_{\pm}$  passing through a stationary ion background of density  $(1-2\epsilon)n$  and electron background of density  $n$ . We consider the symmetrical situation where no zero order

currents exist so that finite  $\beta$  effects may be treated consistently. The temperatures  $T_{\parallel}$  of all components is equal and  $T_{\perp} = 0$  also, for all components. The correct mass ratio  $\mu \equiv m_{+}/m_{-} = 1837$  is used. Some definitions used are:

$$\begin{aligned} \tau &= \frac{T_{\parallel,+}}{T_{\parallel,-}} & \theta &= \frac{k_{\parallel}}{k_{\perp}} & \bar{\omega}_p &= \frac{\omega_p}{\Omega_-} \\ \omega_p &= \frac{4\pi n e^2}{m_-} & \Omega_{\pm} &= \frac{|e| B_0}{m_{\pm} c} & \beta &= \frac{4\pi n T_{\parallel}}{B_0^2} \\ \frac{1}{a_{\pm}} &= k_{\parallel} \tilde{R}_{\parallel,\pm} & \tilde{R}_{\parallel,\pm} &= \frac{\sqrt{2} \tilde{v}_{\parallel,\pm}}{\Omega_{\pm}} & \tilde{v}_{\parallel}^2 &= \frac{T_{\parallel}}{m} \\ \phi &= \angle(\vec{k}, \vec{B}_0) \end{aligned} \quad (1)$$

and quantities without subscripts refer to electrons. Note that  $\theta = 0 \Rightarrow \phi = 90^\circ$ . It is found that the largest growth rates occur for  $\theta \rightarrow 0$  and for  $\bar{\omega}_p \equiv \omega_p/\Omega_- \rightarrow \infty$ .

As we have already<sup>5</sup> found for the  $\omega_r=0$  mode with  $T_{\perp}=0$  (and almost perpendicular propagation) that instability exists for  $\beta > .591$  without any streaming, we decided as a first step to look for marginal growth ( $\omega_i \approx 0$ ) criteria as a function of  $\beta$  for the same mode. These results, given in Figs. 1 and 2 show that the streaming ions lower the  $\beta$  threshold to zero. To explore the minimum ion streaming required for instability we have summarized the results of various curves such as given in Figs. 1 and 2 and have plotted in Fig. 3,  $\tilde{V}_+$  versus  $1/a \equiv k_{\parallel} \tilde{R}_{\parallel}$  for  $\beta \sim 0$ . This shows that  $\tilde{V}_+ > .942$  is needed for instability.

The main new results for the growth rates are given in Fig. 4. These are computer solutions of the exact equations using the Barberio-Corsetti<sup>9</sup> program for the plasma  $Z$  function and a Taylor series expansion up to second order to solve for the complex variable  $\omega = \omega_r + i\omega_i$  as a function of real  $k$ . The equations have been checked by various independent means and also give results consistent with Gaffey et al,<sup>10</sup> in particular his Figs. 1a and 3a. These figures are reproduced as Figs. 5 and 6 below with our added curve and point to show both the correctness and consistency of our equations and code as well as to show that no singularity occurs for  $T_\perp = 0$ . Since the electromagnetic mode occurs only for finite  $\beta$ , while the mode we are discussing occurs also for  $\beta_\parallel \sim 0$ , we see that in general, maximum growth does not occur in the  $k_\parallel \rightarrow 0$  electromagnetic limit considered by Gaffey et al<sup>10</sup>.

From Fig. 4 there are two basic modes. One with  $\omega_r = 0$  has the largest growth rate for  $\epsilon = \frac{1}{2}$  (100% streaming), while the other is near the lower hybrid (LHy) frequency and predominates for  $\epsilon \ll 1$  (very low % streaming). The  $\omega_r = 0$  mode has been considered by Weibel<sup>11</sup> for  $T_\perp = T_\parallel$  and  $\theta^2 a_+^2 = \frac{1}{6}$ . This choice of  $\theta a_+$  (which is not optimized for maximum growth) gives a growth rate of  $.02\Omega_+$  for  $\tilde{V}_+ = 10$  and a maximum growth rate of  $.07\Omega_+$  at  $\tilde{V}_+ = 100$ , much lower than our  $T_\perp = 0$  growth rate. The other mode is new and does not appear in the literature.

As shown in Fig. 4 for the highest curve, the instability is mainly electrostatic (Stix<sup>7</sup> p. 224) and we shall therefore use this electrostatic (ES) equation in our analysis. It is

interesting to note that computer solutions of the exact equations (see Fig. 7) show that the ES limit is indeed approached as  $\beta \rightarrow 0$ , but that as  $\beta$  increases the growth increases. This behavior is contrary to that found in gradient (or drift) waves, where the growth rate decreases as  $\beta$  increases.<sup>12</sup>

The electrostatic equation has been given e.g., by Stix, p.224, for a bi-Maxwellian plasma with streaming. It may be written in the general form,

$$1 + \theta^2 + \sum_j \sum_{n=-\infty}^{\infty} \left( \frac{\omega_p^2}{2} \right) \tilde{T}_n \tilde{A}_n = 0 \quad (2)$$

where

$$\begin{aligned} \tilde{T}_n &\equiv \frac{2e^{-\lambda}}{\lambda} I_n(\lambda) , \quad \tilde{A}_n \equiv -\frac{T_{\perp}}{T_{\parallel}} z' \left( \hat{\zeta}_n \right) - na z \left( \hat{\zeta}_n \right) , \\ \hat{\zeta}_n &\equiv \zeta_n + \tilde{V} , \quad \zeta_n \equiv a(z+n) , \quad z_{\pm} = \frac{\omega}{\Omega_{\pm}} , \quad \tilde{V} = \frac{V}{\sqrt{2} \bar{v}} \end{aligned} \quad (3)$$

and

$$\lambda = \frac{k_{\perp}^2 T_{\perp}}{m \Omega^2} = \left( \frac{1}{2 \theta^2 a^2} \right) \frac{T_{\perp}}{T_{\parallel}} .$$

Each "j" term denotes a particular species, for which the appropriate mass, temperature and stream velocity must be substituted.

Specializing now to our case where all the ions are streaming ( $\epsilon = .5$ ) and no electrons stream, together with the assumptions  $T_{\perp} = 0$  and equal parallel temperatures for all components, we obtain



$$2(1 + \theta^2) + \bar{\omega}_p^{-2} \left[ -az \langle \zeta_1 \rangle + az \langle \zeta_{-1} \rangle - 2\theta^2 a^2 z' \langle \zeta_0 \rangle \right] \\ + \sum_{+, -} \mu \left( \frac{\bar{\omega}_p^{-2}}{2} \right) \left[ -az \langle \zeta_1 \pm \tilde{v} \rangle + az \langle \zeta_{-1} \pm \tilde{v} \rangle - 2\theta^2 a^2 z' \langle \zeta_0 \pm \tilde{v} \rangle \right]_+ = 0 \quad (4)$$

where  $z_{\pm} = \omega/\Omega_{\pm}$  and  $\tilde{v}_{\pm} = v_{\pm}/\sqrt{2} \bar{v}_{\parallel, \pm}$ . The standard notation for the plasma function  $z(\zeta)$  and its derivative  $z'(\zeta)$  are also used, where  $\langle \rangle$  indicates the argument. The  $\pm \tilde{v}$ , indicates a sum over two terms, and hence the  $\frac{1}{2}$  factor. (Note that  $az \equiv \omega/k_{\parallel} \sqrt{2} \bar{v}_{\parallel}$ .)

Largest growth is obtained by letting  $\theta^2 \rightarrow 0$  so that the  $n = 0$  damping terms are zero. Analytic expressions for the marginal stability curves shown in Fig. 3 are now easily obtained from Eq. (4). Using the asymptotic expansion<sup>13</sup> for all the  $z$  functions which is valid if  $a \gg 1$  and  $\tilde{v}_{\pm} \gg 1$ , and assuming  $\bar{\omega}_p^{-2} \rightarrow \infty$  and using  $a_{+} = a_{-}/(\mu\tau)^{1/2}$  with  $\tau = 1$  gives the rightmost curve of Fig. 3, labelled  $\sim a$ . The leftmost curve is obtained using the convergent expansion for the  $z(-a_{+} + \tilde{v}_{+})$  term and is labelled  $\sim a_{+}$ . The results are

$$\frac{1}{a_{-}} = \frac{1}{\mu^{1/2} \tilde{v}_{+}} = \frac{1}{\mu^{1/2} a_{+}}, \quad \frac{1}{a_{-}} = \frac{1}{\tilde{v}_{+}} \quad (5)$$

for the leftmost and rightmost marginal stability curves of Fig. 2 with good accuracy for  $\tilde{v}_{+} > 3$ .

The next step is to obtain the growth rate for the  $\omega_r = 0$  mode. The electron terms are easily simplified [since  $z \ll 1$  (from Fig. 4) and  $a \gg 1$  (from Fig. 3) near maximum growth] giving  $\bar{\omega}_p^{-2} \cdot 2$ . For the ion terms one also uses the asymptotic

expansion since  $\tilde{V}_+ \gg 1$ . They may be further simplified using  $1/a_+ \approx (\mu^{1/2}/\tilde{V}_+) \cdot 1/2$  (from Fig. 3, near maximum growth) so that  $a_+^2 \ll \tilde{V}_+^2$  giving

$$\left[ -az \langle \zeta_1 \pm \tilde{V} \rangle + az \langle \zeta_1 \pm \tilde{V} \rangle \right] \approx \frac{-2a_+^2}{(a_+z_+ \pm \tilde{V}_+)^2 - a_+^2} \approx \frac{-2a_+^2}{(a_+z_+ \pm \tilde{V}_+)^2} \quad (6)$$

Combining these results with Eq. (4) yields (with  $\theta^2 \rightarrow 0$ ),

$$2 + \frac{2\omega_p^2}{\Omega_-^2} = \sum_{+, -} \frac{\omega_{p,+}^2}{(\omega \pm k_{\parallel} V_+)^2} \quad (7)$$

which is the two stream instability equation in the limit  $\Omega \rightarrow \infty$ .

From Stix,<sup>7</sup> p. 113, one easily obtains the growth rate (since  $1/2(2\mu)^{1/2} = .83 \times 10^{-2}$ )

$$\gamma \equiv \frac{\omega_i}{\Omega_-} = .83 \times 10^{-2} \cdot \frac{\bar{\omega}_p}{(1 + \bar{\omega}_p^{-2})^{1/2}} \quad (8)$$

which is only 1% above the maximum ES growth rate of Fig. 4

when  $\bar{\omega}_p \rightarrow \infty$ . This maximum occurs at a wavenumber,  $k_{\parallel} \tilde{R}_{\parallel} \equiv 1/a = (3/8)^{1/2}/\tilde{V}_+ = .612/\tilde{V}_+$  which is only ~10% above the dashed curve of Fig. 3.

The  $\bar{\omega}_p$  dependence indicated by the simple formulae of (8) is validated by computer results (<7% error for  $\bar{\omega}_p \geq .5$ ) using a fairly random sample of points from Fig. 8 including the  $\epsilon = .005(1\%)$  LHy curve.

From Eq. (7) the physical mechanism is clear. The ions see no magnetic field and hence the simple  $\vec{k} \cdot \vec{V} = k_{\parallel} V_+$  denominator term driving the instability. There is no electron Landau damping because the electron mass is effectively increased by the factor  $1/\theta^2$ , but the electrons do contribute an effective

dielectric constant  $K_{\perp} = 1 + \frac{\omega_p^2}{\omega^2}$ , which slows the instability. Thus for the ions, which barely move a gyroradius during the instability,  $\vec{B}_0 = 0$ , while for the electrons it is dominant. Suggestions which led to this result were made by C. S. Liu.<sup>14</sup>

## 1.2 EQUAL PARALLEL AND PERPENDICULAR TEMPERATURES ( $T_{\perp} = T_{\parallel}$ )

We next wish to consider in an approximate way how the instability is stabilized by increasing  $T_{\perp}$ . Using Weibel's<sup>11</sup> results as a guide, we will obtain a simple equation using only  $n = 0, \pm 1$  terms in Eq. (2). After correcting several of his misprints so that in his corrected notation, since  $\gamma^2 \equiv T_{\perp}/T_{\parallel}$

$$\lambda \equiv \lambda_{\perp} \equiv (1/2). \quad (\gamma a k_{\perp} / \Omega_+)^2 = (k_{\perp}^2 / \Omega_+^2) (T_{\perp} / m_+)$$

we find in our notation  $\theta^2 a_+^2 = (1/2\lambda_{\perp}) T_{\perp}/T_{\parallel}$ . (Weibel's growth rates are calculated only for  $\lambda_{\perp} = 3$ ). Since  $\lambda_{\perp} \equiv \lambda_+ = \mu \lambda_-$  if  $\tau = 1$ , assuming that  $\lambda_+ \sim 1$  implies that  $\lambda_- \ll 1$  so the  $n = 0$  electron term in Eq. (3) is unchanged. It may be evaluated by noting that near maximum growth  $a \approx \mu^{1/2} \tilde{V}_+$  [as seen from the Fig. 3 insert and Eq. (5)] while  $|z| = \gamma = \gamma_+/\mu$  and  $\gamma_+ \lesssim .1$  so that  $az \ll 1$  if  $\tilde{V}_+ \ll 500$ . Therefore  $Z'(0) \approx -2$  and the  $n = 0$  electron term is given by the first term of Eq. (9) below.

The  $n = \pm 1$  electron term is also unchanged because the additional  $Z'(\zeta)$  term occurring in Eq. (3) when  $T_{\perp} = 0$  is much smaller than the  $Z(\zeta)$  term by a factor  $1/a^2 \ll 1$  (since from Fig. 3 insert and Eq. (5),  $a = \mu^{1/2} a_+ = \mu^{1/2} \tilde{V}_+ \gg 1$ ). Its value is again  $2\bar{\omega}_p^2$ , much less than the  $n = 0$  term in Eq. (4).

The ion  $n = 0$  term has a factor  $\tilde{T}_0 \equiv e^{-\lambda} I_0(\lambda_+)$ , but is otherwise as given in Eq. (4). It too is small and much less than the  $n = 0$  electron term by the factor  $2\tilde{T}_0/\tilde{V}_+^2$ .

Considering lastly the  $n = \pm 1$  ion term shows that the  $z' \langle \zeta \rangle$  term is smaller than the  $z \langle \zeta \rangle$  term by a factor  $1/a_+^2 \approx 1/\tilde{V}_+^2 \ll 1$  and can be neglected. Adding the factor  $\tilde{T}_1 \equiv 2e^{-\lambda} I_1(\lambda)/\lambda$  and using Eq. (6) gives the desired terms after summing over both streams. Since  $\lambda_+ \sim 1$  is not too large, neglect of  $n > 1$  ion terms in Eq. (2) should not be a bad approximation and we obtain the desired equation,

$$\left( \frac{T_1}{T_{\parallel} \lambda_+} \right) 2\mu\omega_p^{-2} + \mu\omega_p^{-2} \tilde{T}_1 \left[ \frac{-a_+^2}{(a_+ z_+ \pm \tilde{V}_+)^2} - a_+^2 \right] = 0 \quad (9)$$

which is independent of ion mass.

Equation (9) is easily solved and for  $T_1 = T_{\parallel}$  there is instability when  $1/\tilde{V}_+ < 1/a_+ < 1.18/\tilde{V}_+$  with  $\gamma_{+,m} \approx .09$ . This is rather close to the instability range found by Weibel, as obtained from his Fig. 1,  $1.05/\tilde{V}_+ < 1/a_+ < 1.17/\tilde{V}_+$  for  $\tilde{V}_+ > 10$ . It is also close and somewhat higher than Weibel's maximum growth,  $\gamma_{+,m} \approx .07$ , obtained by him for  $V_+ \approx 100$ , but much higher than his value  $\gamma_{+,m} \approx .022$  obtained by him for  $\tilde{V}_+ \approx 10$ . The  $\lambda_+$  dependence of Eq. (9) is  $\lambda \tilde{T}_1 = e^{-\lambda} I_1(\lambda)$  which is rather insensitive to the choice of  $\lambda$  ( $=\lambda_+$ ). Thus Weibel's choice  $\lambda_+ = 3$  or our choice  $\lambda_+ = 1$  hardly affects the result. It should however be noted that for the exactly perpendicular EM mode, there is a large difference in growth rates between the  $\lambda = 1$  and  $\lambda = 3$  case (see Fig. 6). Thus exact calculation is necessary.

In the region where  $T_1 \approx T_{\parallel}$ , the growth rate from Eq. (9) is  $\propto T_{\parallel} / T_1$ , but becomes  $\propto (T_{\parallel} / T_1)^{1/2}$  when  $T_{\parallel} / T_1 \gg 3$  (when  $\lambda \approx 1$ ). Moreover, the large growth rate given by Eq. (8)

( $\gamma_+ \approx 15\Omega_+$ ) which is about 230 times larger than Weibel's maximum ( $\gamma_+ \approx .066 \Omega_+$ ) is obtained from Eq. (9) only for  $T_\perp / T_\parallel < 1/2\mu \approx .27 \times 10^{-3}$ . This suggest that our growth rate results for the electrostatic case are relatively sensitive to the correct  $T_\perp / T_\parallel$  ratio. The instability threshold, which is a more important quantity, is much less sensitive. We obtain  $\tilde{V}_+ > .94$ , while Weibel<sup>11</sup> obtains (from his Fig. 1 or our Fig. 3 insert) that  $\tilde{V}_+ > 8$ . for instability.

We next wish to show that by choosing the value of  $\theta^2 a^2$  in Eq. (4), appropriately, we can simulate the  $T_\perp = T_\parallel$  case using our  $T_\perp = 0$  computer program. As mentioned earlier, by definition (when  $T_\perp = T_{\parallel,+} = T_{\parallel,-}$ )

$$\theta^2 a^2 = \left( \frac{\mu}{2\lambda_+} \right) \frac{T_\perp}{T_\parallel} = \frac{\mu}{2\lambda_+} \quad (10)$$

and using this value of  $\theta^2 a^2$  (for given  $\lambda_+$ ), Eq. (4) is similar to Eq. (9) aside from the  $\tilde{T}$  factor multiplying the ion  $n = \pm 1$  terms, if we use the same assumptions used to obtain Eq. (9), i.e.,  $a_+ \gg 1$ ,  $\tilde{V}_+ \gg 1$  etc. Now since there are only two dominant terms in Eq. (9), one, the  $n = 0$  electron damping term with the  $\theta^2 a^2$  factor and the other the  $n = \pm 1$  ion driving term, with the  $\tilde{T}_1$  factor, we see that we can absorb the  $\tilde{T}_1$  factor in the  $\theta^2 a^2$  term if we redefine it as [c.f. Eq. (10)],

$$\theta^2 a^2 = \frac{\mu}{2\lambda_+ \tilde{T}_1} = \frac{\mu}{4e^{-\lambda_+} I_1(\lambda_+)} \approx \frac{\mu}{.88} \quad (11)$$

so that

$$\theta a_+ \approx \frac{1}{(.88)^{1/2}} = 1.07 \quad (12)$$

(We have used the maximum value of  $e^{-\lambda_+} I_1(\lambda_+) \approx .22$ , occurring for  $\lambda_+ \approx 1$ , where the maximum is quite broad).

Thus, by using a value of  $\theta \neq 0$ , given by  $\theta a_+ = 1.07$ , we expect to approximately reproduce the  $T_\perp = T_\parallel$  case with our computer program. This means that instead of using  $k_\perp \sim \infty$ , we use finite  $k_\perp$  ( $\theta \equiv k_\parallel/k_\perp$ ). This reduces slightly the maximum growth rate obtained from Eq. (9), i.e., instead of  $\gamma_+ \approx .09$  we find for  $\tilde{V}_+ = 10$ ,  $\gamma_+ \approx .079$ , somewhat closer to Weibel's value. We summarize some of our results in Table I.

TABLE I.

$\beta$	$\theta$	$1/a$	$\theta a_+$	$\gamma_{m,+}$
.1	.084	$.194 \times 10^{-2}$	1.02	.42
.01	.091	$.208 \times 10^{-2}$	1.02	.34
.001	.116	$.266 \times 10^{-2}$	1.02	.113
.0001	.12	$.275 \times 10^{-2}$	1.02	.081
.00001	.12	.275	1.02	.079
ES	.12	.275	1.02	.079

Table I. Some results for maximum growth rates as a function of 'a' for  $\tilde{V}_+ = 10$ ,  $\tilde{\omega}_p = 100$ , all protons streaming ( $\epsilon = \frac{1}{2}$ ) and  $\tau = 1$  ( $T_+ = T_-$ ) for the  $\omega_r = 0$  mode. The term  $\gamma_{m,+}$  means the maximum value of  $\gamma_+$  as a function of  $1/a$  for fixed  $\theta a_+$ . The growth rates for  $\theta a_+ = 1.07$  are only 1% lower.

The most interesting feature is the remarkable sensitivity of the growth rate to  $\beta$ . Note that only for  $\beta \leq 10^{-5}$  do we get within 1% of the growth rate given by the electrostatic (ES) equation. When  $\beta = .1$  the growth rate is  $5.3\times$  larger than the value from the ES equation. Figures 3 and 7 suggest what is occurring. From Fig. 3 we see that as  $T_{\perp}$  increases toward the value  $T_{\parallel}$ , the range of unstable wave numbers narrows and the peak growth occurs at smaller  $k_{\parallel} \tilde{R}_{\parallel} \equiv 1/a$ . The minimum  $k_{\parallel}$  for instability remains essentially unchanged and only the maximum  $k_{\parallel}$  for instability decreases. Comparing Eqs. (10) and (4) we see that for a given  $k_{\parallel} \tilde{R}_{\parallel} \equiv 1/a$ , increasing  $T_{\perp}$  means increasing  $\theta$ , which means increasing the  $n = 0$ , electron damping term. As  $\theta$  is increased from zero (for zero  $T_{\perp}$ ), the wave vector,  $\vec{k}$  is oriented more along the field line and hence is more subject to the damping by the electrons which are free to move along the field line and rather constrained perpendicular to it. The larger values of  $k_{\parallel} \tilde{R}_{\parallel} = 1/a$  values, i.e. shorter wavelengths, are more easily damped, as occurs in the typical longitudinal oscillations (q. v. Jackson,<sup>15</sup> Fig. 3). Note that  $k_{\parallel}$  and  $k_{\perp}$  are the independent variables to be adjusted for maximum growth, but we have instead used  $\theta$  and 'a', which are functionals of  $k_{\parallel}$  and  $k_{\perp}$ , as the independent variables. Thus, fixing the value of  $\theta a_{+}$  while allowing 'a', to vary, means fixing the value of  $k_{\perp}$ , so the problem is not overdetermined.

The above is a sketch of the behavior of the damping term. To understand the  $\beta$  dependence shown in Table I, we note that Fig. 7 shows that for smaller  $1/a$  values, that the growth rates

are larger for larger  $\beta$ . Since this is precisely the region of maximum growth for  $T_{\perp} \approx T_{\parallel}$ , the growth is sensitive to the value of  $\beta$ . We conjecture that the reason is that for smaller 'k', i.e., larger  $\lambda$  (wavelength), for the same charge density, the current is larger, and hence magnetic effects are more important. Alternatively, from Maxwell's Eqs.,  $\nabla \times B = 4\pi J$  (neglecting the displacement current term), or  $B \sim 4\pi J/k$ , again showing that magnetic field effects are more important for small  $k_{\parallel}$ . (This argument is of necessity qualitative since  $k_{\perp} \gg k_{\parallel}$ .)

It is interesting to note, from Table I, that the rapid change in  $\gamma_{m,+}$  occurs for  $.001 < \beta < .01$ , which is the typical Tokamak<sup>16</sup> regime. The importance of finite  $\beta$  has been noticed by Forslund<sup>17</sup> et al, in a related example. The main difference is that they treated streaming electrons in an ion background, so that there is a zero order magnetic field due to the zero order current whose effect they neglected. This makes their finite  $\beta$  effects suspect. Since there is no zero order current in our symmetrical streaming case, the finite  $\beta$  effects we have found seem more persuasive, even though we have only modelled the  $T_{\perp} = T_{\parallel}$  case.

### 1.3 DISCUSSION

The importance of  $k_{\perp}$  instabilities has been first pointed out by Drummond and Rosenbluth.<sup>18</sup> In their paper they found that a relative streaming velocity of ions and electrons (when  $T_{+} = T_{-}$ ) of only  $\sim 15$  times the ion thermal velocity ( $\sqrt{2} \bar{v}_{+}$ ) is needed



for instability. This is  $\sim 1/3$  the critical velocity for the  $k_{\parallel}$  instability which requires that the relative streaming velocity be greater than .95 the electron thermal velocity.<sup>15</sup> Thus the required streaming velocity is about 3 times smaller for the  $k_{\perp}$  instability relative to the  $k_{\parallel}$  instability. More detailed numerical work by Lominadze and Stepanov<sup>19</sup> (reviewed by Mikhailovskii,<sup>20</sup> p. 221) shows that for deuterium the threshold is  $23 \times (\sqrt{2} \bar{v}_+)$  when  $T_+ = T_-$ , with a  $\mu^{1/2}$  dependence, so their result agrees with Drummond and Rosenbluth's<sup>18</sup> value of 15 for Hydrogen, ( $\mu=1837$ ) whose mass dependence formulae is however  $\sim (\ln \mu)^{1/2}$ . Weibel<sup>11</sup> finds no mass dependence in his case where there are counterstreaming ions with an electron background, which is understandable because the instability is driven by an ion-ion interaction, not an electron-ion interaction.

We have also found the Drummond-Rosenbluth (D-R) ion cyclotron instability in our counterstreaming ion case. We have partially explored only the  $\beta_{\parallel} \approx .1$  region and we find that instability occurs in repeated bands in a three dimensional, space with  $\tilde{v}_+$ ,  $1/a_+$ , and  $\theta$  the parameters, in the band with smallest  $1/a_+$  values, (see Figs. 3 and 7) instability occurs for  $1.4 < \tilde{v}_+ < 1.95$ ,  $.05 < 1/a_+ < .02$  and  $.01 < \theta < .16$ , approximately. It is not yet clear why the growth for this mode stops when  $\tilde{v}_+ > 2.$ , but it apparently shifts to another band with larger values of  $1/a_+$ . Perhaps the other ion stream and the finite  $\beta$  play a role. In the region of maximum growth where  $\tilde{v}_+ = 1.8$ , we find  $b_+ \equiv \omega_r/\Omega_+ = .14$ ,  $\gamma_+ = .01$  and  $1/a_+ = .13$ , relatively close to the values expected from Drummond and Rosenbluth<sup>18</sup> for  $\tilde{v}_+ > 15$ , i.e.,

$b_+ = 1.2$ ,  $\gamma_+ = .013$  and  $1/a_+ = .08$  ( $\gamma_+$  is actually calculated from Eq. (8) of D-R with  $\tilde{V}_+ = 1.8$ ).

Thus the growth is clearly larger than expected from D-R because  $T_+ = 0$  and finite  $\beta$  effects. Since the  $\omega_r = 0$  and  $\omega_r \neq 0$  D-R instabilities coexist we can obtain the self-consistent finite  $\beta$  corrections to the D-R instability by including the counterstreaming ion beam. Examination of Fig. 7, shows that finite  $\beta$  effects become more important for  $1/a$  small and hence we expect these effects to be more important for the D-R,  $\omega_r \neq 0$  mode than for the  $\omega_r = 0$  mode which we calculated in Table I.

## 2. LOWER HYBRID INSTABILITY

When the amount of streaming ions is decreased i.e. when  $\epsilon$  drops below  $\frac{1}{2}$ , then the dominant instability becomes one with real part near the lower hybrid frequency, i.e.

$\omega_r \approx (\Omega_+ \Omega_-)^{1/2} = \Omega_-/\mu^{1/2}$ . This is shown in Fig. 4. The numbers on the curves give  $\tilde{\alpha} \equiv \omega_r \mu^{1/2}/\Omega_-$ , i.e. the real frequency in units of the lower hybrid frequency.

To obtain an analytic solution, for the parameters shown in Fig. 4, we again use Eq. (4). The  $n = \pm 1$  electron terms again give  $\tilde{\omega}_p^2 \cdot 2$  because  $a \gg 1$  and  $z \ll 1$ . (The  $LH_y$  mode occurs for  $1/a$  values just to the right of the  $\omega_r = 0$  mode marginal stability curve shown in Fig. 3, i.e.  $\tilde{V}_+ \approx a$  or  $k_{||}V_+/\Omega_- \approx 1$ ). The  $n = 0$  electron and ion terms are again neglected since we assume  $T_+ = 0$  and  $\theta \approx 0$ , so that we turn next to the ion  $n = \pm 1$  terms. There are now two sets of these

ion terms. One set, describing the streaming ions, has the factor  $\epsilon$  [instead of  $1/2$  used in Eq. (4)], while the other set describing the stationary ions has the factor  $1-2\epsilon$ , but is otherwise the same as the appropriate ion term given in Eq. (4) (with  $\tilde{V}_+ = 0$ , of course). For both sets of terms we use Eq. (6) so that collecting the various terms, i.e. the  $n = \pm 1$  electron and  $n = \pm 1$  ion, Eq. (4) becomes (with  $\hat{V}^2 \equiv \tilde{V}_+^2/a_+^2 = k_{\parallel}^2 V_+^2/\Omega_+^2$ ),

$$\frac{z_+^2}{\omega_p^2} + 2 + \mu(1-2\epsilon) \left( \frac{-2}{z_+^2} \right) + \frac{\mu\epsilon(-4)(z_+^2 + \hat{V}^2)}{(z_+^2 - \hat{V}^2)^2} = 0. \quad (13)$$

It is easily verified that with  $\epsilon = 1/2$  this is the same as Eq. (7), and that when  $\hat{V} = 0$ , the  $\epsilon$  terms cancel.

We now wish to write Eq. (13) in a dimensionless form more convenient for obtaining a solution. Thus we write

$$z_+^2 = \tilde{\mu} (\alpha + i\beta) \text{ where } \tilde{\mu} \equiv \mu \frac{\omega_p^2}{1 + \omega_p^2} \text{ and } \hat{V}^2 = \tilde{\mu} \delta \quad (14)$$

with  $\alpha$  and  $\beta$  real. With these substitutions Eq. (13) becomes

$$1 - \frac{(1-2\epsilon)}{\alpha + i\beta} - \frac{2\epsilon (\alpha + i\beta + \delta)}{(\alpha + i\beta - \delta)^2} = 0 \quad (15)$$

which is a cubic in the variable  $\alpha + i\beta$ . A good approximation to the solution may be obtained by assuming that  $\epsilon \ll 1$ , i.e. low density of streaming ions, together with the ordering,

$$x \equiv \delta - \alpha \sim \tilde{\lambda}, \quad \epsilon \sim \tilde{\lambda}^3, \quad \tilde{\mu} \sim \tilde{\lambda} \text{ and } \alpha \sim \delta \sim 1, \quad (16)$$

where  $\tilde{\lambda}$  is a small parameter. Then to order  $\tilde{\lambda}^3$  we obtain

$$(-x + i\tilde{\beta})^2 \left[ 1 - \frac{1}{\alpha} (1 - i\tilde{\beta}) \right] - 4\epsilon = 0.$$

The real and imaginary parts of this equation are

$$(x^2 - \tilde{\beta}^2) \left( 1 - \frac{1}{\alpha} \right) + 2x\tilde{\beta}^2 - 4\epsilon = 0,$$

$$i\tilde{\beta} \left[ -2x \left( 1 - \frac{1}{\alpha} \right) + (x^2 - \tilde{\beta}^2) \right] = 0,$$

to lowest order, i.e. order  $\tilde{\lambda}^3$ . Eliminating  $\alpha$  gives a quadratic in  $\tilde{\beta}^2$  which can be solved to give

$$\tilde{\beta}^2 = -x^2 + 2(2\epsilon x)^{1/2}, \quad \alpha = 1 + x - \left( \frac{2\epsilon}{x} \right)^{1/2}. \quad (17)$$

Returning to Eq. (14) we find to lowest order,

$$z_+ \equiv b_+ + i\gamma_+ \approx \mu^{1/2} \left( \alpha^{1/2} + \frac{i\tilde{\beta}}{2} \right).$$

Thus the maximum growth rate is found by maximizing  $\tilde{\beta}$  in Eq. (17) which gives finally,

$$\begin{aligned} \gamma_{+,m} &= \mu^{1/2} \frac{\tilde{\beta}_m}{2} = \frac{3^{1/2}}{2^{4/3}} \epsilon^{1/3} \mu^{1/2} \frac{\bar{\omega}_p}{(1 + \bar{\omega}_p^2)^{1/2}} \\ b_{+,m} &\equiv \frac{\omega_{r,m}}{\Omega_+} = (\mu \alpha)^{1/2} = \left( 1 - \frac{\epsilon^{1/3}}{2^{4/3}} \right) \mu^{1/2} \frac{\bar{\omega}_p}{(1 + \bar{\omega}_p^2)^{1/2}}. \end{aligned} \quad (18)$$

In order to compare these results with the computer results of Fig. 4, we rewrite them in the following form (with  $\bar{\omega}_p \gg 1$ ), the growth rate in units of the electron gyrofrequency and the real part of  $\omega$  in units of the lower hybrid frequency. Thus

$$\gamma_m = \frac{3^{1/2}}{2^{4/3}} \frac{1}{\mu^{1/2}} \epsilon^{1/3} = 1.6 \times 10^{-2} \epsilon^{1/3},$$

$$\tilde{\alpha}_m \equiv \frac{\omega_{r,m} \mu^{1/2}}{\Omega_-} = 1 - \frac{\epsilon^{1/3}}{2^{4/3}} = 1 - .4\epsilon^{1/3}. \quad (19)$$

Comparing these results with those given in Fig. 4, we see that Eq. (19) gives for  $\epsilon=.005$  ( $\epsilon^{1/3} \approx .17$ ),  $\gamma_m = .27 \times 10^{-2}$ ,  $\tilde{\alpha}_m = .93$  which is rather close to the graph values of  $\gamma_m \approx .23 \times 10^{-2}$  and  $\tilde{\alpha}_m \approx .94$ . Note too that  $10^{1/3} = 2.16$ . Thus the simple formulae in Eq. (19) are rather accurate.

The dependence of the growth rate as given in Eq. (18), on the factor  $\bar{\omega}_p/(1+\bar{\omega}_p^2)^{1/2}$  is also well reproduced by the growth rate results shown in Fig. 8 (the lowest curve).

Since the threshold value of  $\tilde{V}_+$  from Fig. 4 is  $\tilde{V}_+ > 3$  (for  $\epsilon=.005$  and  $T_\perp = 0$ ), we expect the threshold of this instability to be also higher than the  $\omega_r = 0$  mode when  $T_\perp = T_\parallel$ . The exact value awaits a more exact calculation.

## 2.1 DISCUSSION

A perpendicular mode similar to that described by Eq. (18) has been found experimentally<sup>21</sup> and was described theoretically by Mikhailovskii.<sup>22</sup> In their case where

$\bar{\omega}_{p,+} = \mu^{1/2} \bar{\omega}_p \sim 1$ , but  $\bar{\omega}_p \ll 1$ , Eq. (18) gives for  $\omega$  at maximum growth,  $\omega_m \equiv \omega_{r,m} + i \omega_{i,m}$ , the values

$$\omega_{i,m} = \frac{3^{1/2}}{2^{4/3}} \epsilon^{1/3} \omega_{p,+}$$

$$\omega_{r,m} \approx \omega_{p,+} \quad (20)$$

which are the same equations given by Mikhailovskii.<sup>22</sup> In this region of small  $\bar{\omega}_p$ ,  $\gamma \sim \bar{\omega}_p$  and is the linear region shown in Fig. 8. For  $\beta$  sufficiently small it is possible to consider  $\bar{\omega}_p$  sufficiently small, so that  $\bar{\omega}_{p,+}$  ( $\bar{\omega}_{p,+} = \mu^{1/2} \bar{\omega}_p$ ) becomes small. For very small  $\bar{\omega}_{p,+} \equiv \omega_{p,+}/\Omega_+$ , i.e. sufficiently large B field, Gabovich et al<sup>21</sup> have shown that the instability is stabilized. Their range of  $\epsilon$  was  $1/2 > \epsilon > .02$  with  $\tilde{V}_+ > 30$ . There is however no clear statement of the minimum  $\tilde{V}_+$  needed for instability and since their maximum  $\bar{\omega}_p \approx .1$  was small by our criteria, it is likely that the minimum  $\tilde{V}_+$  is also smaller when  $\bar{\omega}_p$  is larger.

We note that the agreement of Eq. (20) with the formulae of Mikhailovskii<sup>22</sup> shows that for the  $\omega_r \neq 0$  mode, only one beam is interacting with the plasma. Clearly more work is necessary to establish the critical velocity for instability when  $T_\perp = T_\parallel$  and the electron temperature is higher than the ion temperature.

#### ACKNOWLEDGMENT

I wish to thank P. H. Rutherford and T. H. Stix for their support and encouragement of this work, for several helpful discussions and for making the facilities of Princeton University available. I also wish to thank C. S. Liu for his interest and invaluable suggestions, H. L. Berk for helpful comments and L. A. Ferrari for his support of this work at Queens College.

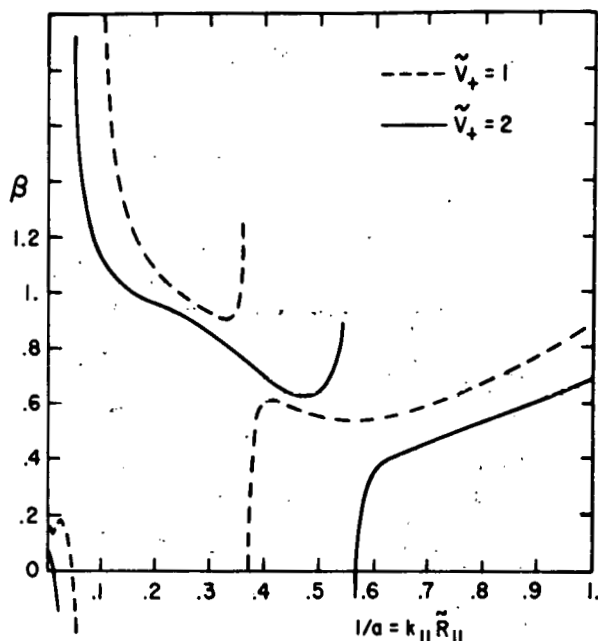
This work was supported by the United States Energy Research and Development Administration Contract E(11-1)-3073.

REFERENCES

- <sup>1</sup>H. P. FURTH and D. L. JASSBY, Phys. Rev. Lett., 32, 1176 (1974) q.v. for earlier references.
- <sup>2</sup>R. M. KULSRUD and D. L. JASSBY, Princeton Plasma Physics Laboratory Report MATT-1114 (1975).
- <sup>3</sup>F. H. TENNEY, private communication.
- <sup>4</sup>J. A. ROME, J. D. CALLEN and J. F. CLARKE, Nucl. Fusion 14, 141 (1974).
- <sup>5</sup>R. W. LANDAU, J. Plasma Phys., (1975) to be published.
- <sup>6</sup>R. W. LANDAU, Phys. Rev., submitted (1975).
- <sup>7</sup>T. H. STIX, The Theory of Plasma Waves, (McGraw Hill, N. Y., 1962) 188-193.
- <sup>8</sup>R. W. LANDAU and S. CUPERMAN, J. Plasma Phys. 6, 495 (1971).
- <sup>9</sup>P. BARBERIO - CORSETTI, Princeton Plasma Physics Laboratory Report MATT-773 (1970).
- <sup>10</sup>J. D. GAFFEY, W. B. THOMPSON and C. S. LIU, J. Plasma Phys., 7, 189 (1972).
- <sup>11</sup>E. S. WEIBEL, Phys. Fluids 13, 3003 (1970).
- <sup>12</sup>A. B. MIKHAILOVSKII, Theory of Plasma Instabilities (Consultants Bureau, N. Y., 1974), Vol. 2, pp 62,63. c.f. N. A. KRALL, Advances in Plasma Physics (Wiley, N. Y. 1968), Vol. 1, Eq. (59), which evidently has a misprint, i.e.  $\gamma \sim \beta^{-1/2}$  not  $\gamma \sim \beta^{3/2}$ .
- <sup>13</sup>B. D. FRIED and S. D. CONTE, The Plasma Dispersion Function (Academic Press, N. Y. 1961).
- <sup>14</sup>C. S. LIU, private communication.

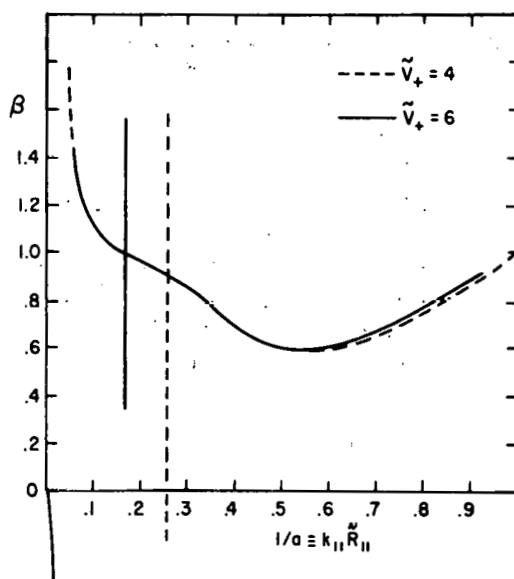


- <sup>15</sup>J. D. JACKSON, Plasma Physics (J. Nucl. Energy, Part C) 1, 171 (1960).
- <sup>16</sup>L. A. ARTSIMOVICH, Nucl Fusion 12, 215 (1972).
- <sup>17</sup>D. W. FORSLUND, C. F. KENNEL and J. M. KINDEL, UCLA, Los Angeles, California, Report R-87, Feb. 1971 (unpublished).
- <sup>18</sup>W. E. DRUMMOND and M. N. ROSENBLUTH, Phys. Fluids, 5, 1507 (1962).
- <sup>19</sup>D. G. LOMINADZE and K. N. STEPANOV, Sov. Phys.-Tech Phys. 9, 1408 (1965), [Zh. Tekh. Fiz. 34, 1823 (1964)].
- <sup>20</sup>A. B. MIKHAILOVSKII, *ibid*, Vol. 1,
- <sup>21</sup>M. D. GABOVICH, A. A. GONCHAROV, V. PORITSKII and I. M. PROTSENKO, Sov. Phys. JETP 37 655 (1973). [Zh. Eksp. Teor. Fiz. 64, 1291 (1973)].
- <sup>22</sup>A. B. MIKHAILOVSKII, *ibid* Vol. 1, p. 69.



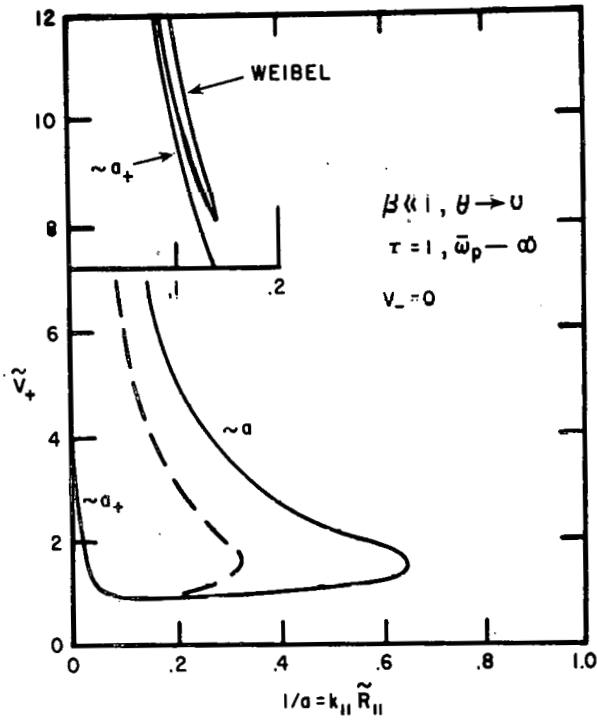
752137

Fig. 1. A plot of marginal stability for  $T_+ = T_-$ ,  $\theta \sim 0$  and  $\bar{\omega}_p \equiv \omega_p / \Omega_- \sim \infty$  for the  $\omega_r = 0$  mode. The minimum, near  $\beta = .591$  exists also for no streaming.<sup>5</sup> In the  $k_{||} \rightarrow 0$  limit,  $\beta = .25$  for  $\tilde{V}_+ = 1$  and  $\beta = .01$  for  $\tilde{V}_+ = 2$ , which gives the marginal stability values for the EM instability.<sup>10</sup>



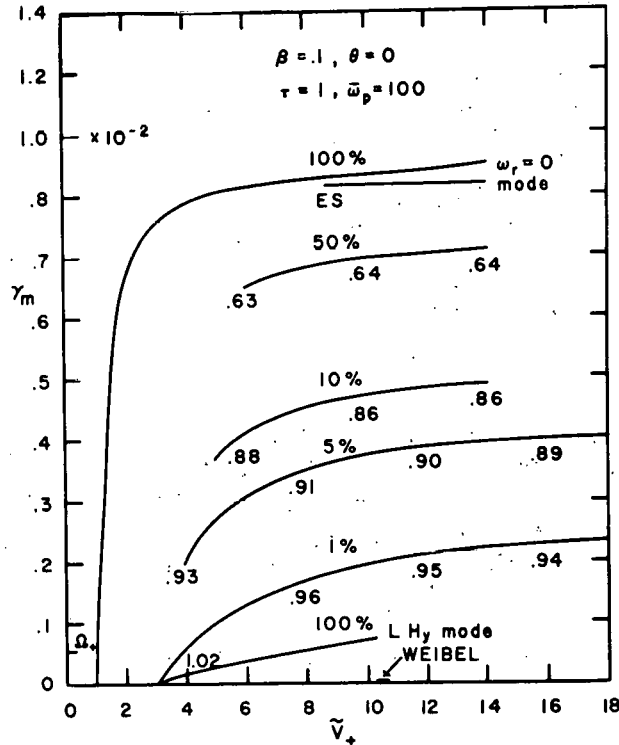
752136

Fig. 2. Marginal stability values as in Fig. 1, but for  $\tilde{V}_+ = 4$  and  $6$ . In the  $k_{||} \rightarrow 0$  limit,  $\beta = .0294$  for  $\tilde{V}_+ = 4$  and  $\beta = .0135$  for  $\tilde{V}_+ = 6$ . The ordinate is  $\beta = 4\pi n T_{||} / B_0^2$  where  $n$  refers to all the ions or electrons.



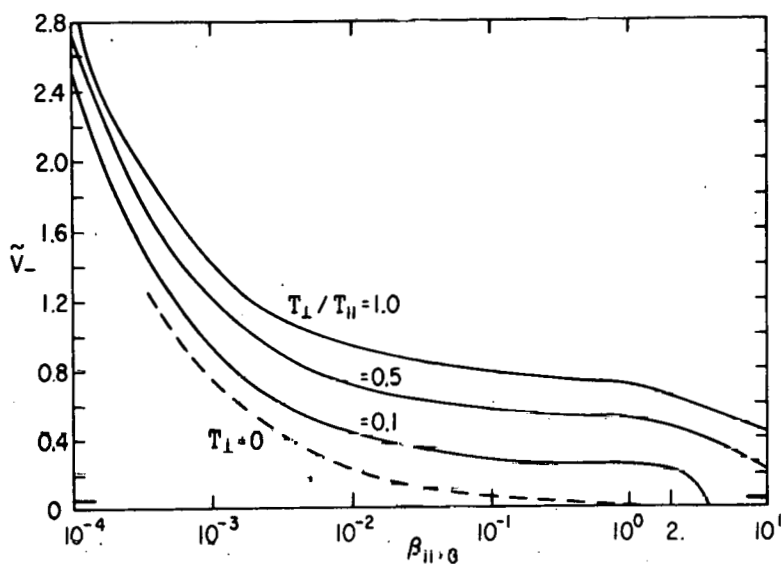
752144

Fig. 3. Marginal stability curves for the parameters indicated for  $T_{\perp} = 0$ . The curves are  $\tilde{V}_+ \approx a_+$  and  $\tilde{V}_+ \approx a$ , valid for  $\tilde{V}_+ > 3$ . Values of 'a' for maximum growth for  $\beta = .1$  are given by the dashed curve. The horizontal axis in the insert is labelled in units of  $1/a_+ = \mu^{1/2}/a$  while the curve gives Weibel's<sup>11</sup> marginal stability limits obtained from his Fig. 1.



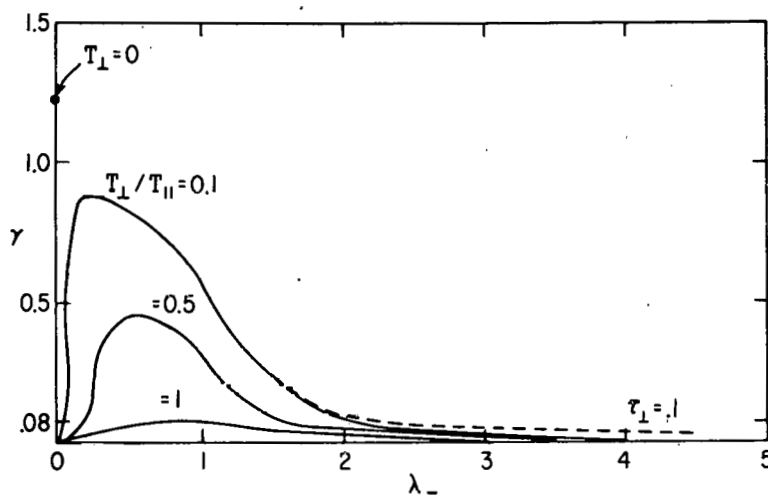
752141

Fig. 4. Maximum growth rates ( $\gamma_m \equiv \omega_i / \Omega_-$ ) obtained for optimum 'a' and  $\theta$ . Optimum  $\theta \sim 0$  for all curves except the LH<sub>y</sub> curve for which  $.12 < \theta < .22$  depending on  $\tilde{v}_+$ . ( $\theta = .12$  corresponds to  $\tilde{v}_+ = 10$ ). ES denotes electrostatic solution ( $\beta \sim 0$ ) while 'Weibel', denotes his<sup>11</sup> maximum growth from his Fig. 1. The % numbers indicate percent of streaming ions. ( $2 \epsilon \times 100 = \%$ ). The numbers under the curves give  $\tilde{\alpha} \equiv \omega_r \mu^{1/2} / \Omega_-$  i.e.  $\omega_r$  in units of  $(\Omega_+ \Omega_-)^{1/2}$ .



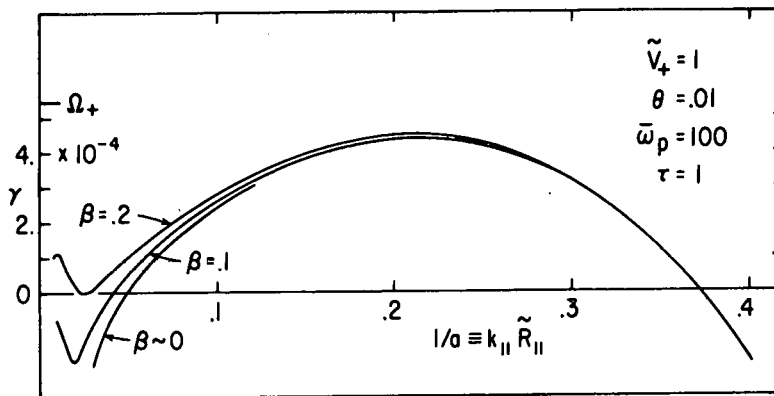
752142

Fig. 5. Marginal stability for the EM mode ( $k_\parallel \rightarrow 0$  limit) from Fig. 1a of Gaffey, et al<sup>10</sup> together with our  $T_\perp = 0$  dashed curve. Here  $V_+ = V_-$ ,  $\beta_{||,G} = 2\beta = 8\pi n T_\parallel / B^2$  and  $T_{\perp,+} = T_{\perp,-}$ . For  $\tilde{V}_- \rightarrow 0$ , our dashed curve approached  $\beta_{||,G} = 2$ .



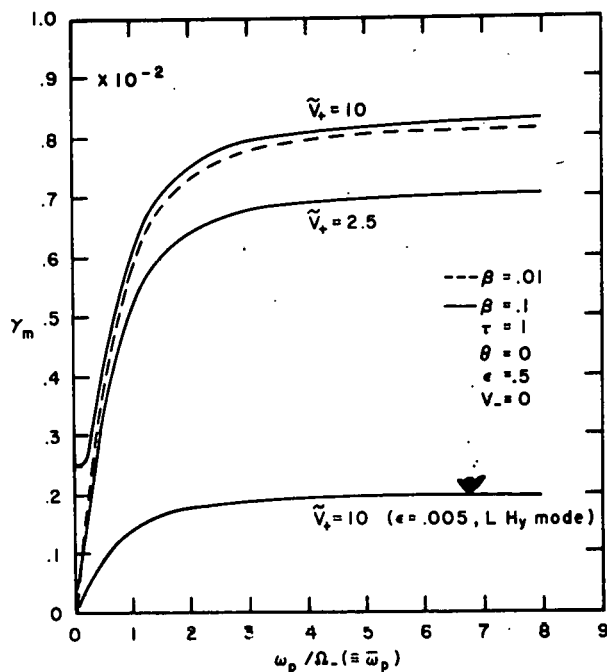
752145

Fig. 6. Growth rates as a function of  $\lambda_- = (k_\perp^2 / \Omega_-^2) (T_\perp / m_-)$  from Gaffey et al,<sup>10</sup> Fig. 3, for  $\beta_{||,G} = 2\beta = 1$ ,  $\tilde{V}_- = 1.414$ ,  $\bar{\omega}_p = 10$ ,  $\tau_\perp \equiv T_{\perp,+} / T_{\perp,-} = 1$  and  $V_+ = V_-$ . (The dashed curve is for  $\tau_\perp = .1$ ). The  $T_\perp = 0$  point is from our code for  $\bar{\omega}_p = 100$ .



752139

Fig. 7. Growth rates for various  $\beta$  for  $T_{\perp} = 0$  and  $v_{\perp} = 0$ , near marginal stability. The  $\Omega_+$  dash indicates where  $\omega_i = \Omega_+$ . The  $LH_y$  mode joins the upper end of the  $l/a$  region and the Drummond-Rosenbluth mode, the lower end.



752140

Fig. 8. Maximum growth rates ( $\gamma_m \equiv \omega_{i,m}/\Omega_-$ ) obtained for optimum  $l/a$ . The difference between the  $\beta = 0.1$  and  $\beta = 0.01$  curves for the  $LH_y$  mode is too slight to show up. Since  $\beta = (\bar{\omega}_p \bar{v}_{\parallel}/c)^2$  values of  $\bar{\omega}_p^2 < \beta$  are unphysical.

#### NOTICE

This report was prepared as an account of work sponsored by the United States Government. Neither the United States nor the United States Atomic Energy Commission, nor any of their employees, nor any of their contractors, subcontractors, or their employees, makes any warranty, express or implied, or assumes any legal liability or responsibility for the accuracy, completeness or usefulness of any information, apparatus, product or process disclosed, or represents that its use would not infringe privately owned rights.